

Feature-selective Attention in Frontoparietal Cortex: Multivoxel Codes Adjust to Prioritize Task-relevant Information

Jade Jackson, Anina N. Rich, Mark A. Williams, and Alexandra Woolgar

Abstract

Human cognition is characterized by astounding flexibility, enabling us to select appropriate information according to the objectives of our current task. A circuit of frontal and parietal brain regions, often referred to as the frontoparietal attention network or multiple-demand (MD) regions, are believed to play a fundamental role in this flexibility. There is evidence that these regions dynamically adjust their responses to selectively process information that is currently relevant for behavior, as proposed by the “adaptive coding hypothesis” [Duncan, J. An adaptive coding model of neural function in prefrontal cortex. *Nature Reviews Neuroscience*, 2, 820–829, 2001]. Could this provide a neural mechanism for feature-selective attention, the process by which we preferentially process one feature of a stimulus over another? We used multivariate pattern analysis of fMRI data during a perceptually challenging categorization task to in-

vestigate whether the representation of visual object features in the MD regions flexibly adjusts according to task relevance. Participants were trained to categorize visually similar novel objects along two orthogonal stimulus dimensions (length/orientation) and performed short alternating blocks in which only one of these dimensions was relevant. We found that multivoxel patterns of activation in the MD regions encoded the task-relevant distinctions more strongly than the task-irrelevant distinctions: The MD regions discriminated between stimuli of different lengths when length was relevant and between the same objects according to orientation when orientation was relevant. The data suggest a flexible neural system that adjusts its representation of visual objects to preferentially encode stimulus features that are currently relevant for behavior, providing a neural mechanism for feature-selective attention. ■

INTRODUCTION

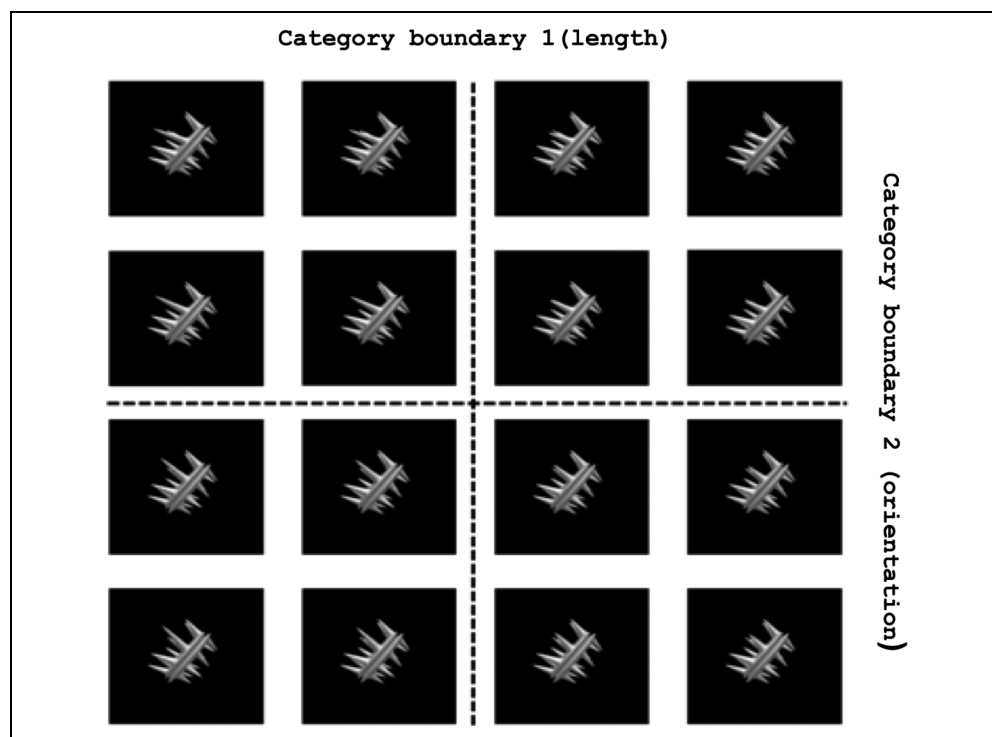
We live in a complex dynamic environment where the behavioral relevance of different sensory input changes rapidly. To function successfully, we need a cognitive system that can select what is currently relevant, ignore distraction, and update its responses in accordance with events in the world. The selection of relevant information can be specific to different features of visual objects depending on the current goal. For example, if I am looking for my blue cup among other cups, color is the relevant dimension. When I find my cup and reach to pick it up, other features of the cup are now relevant (e.g., orientation). Following Chen, Hoffmann, Albright, and Thiele (2012), we refer to the process of attending to and making a decision about one feature of an object, while ignoring other features of that object, as feature-selective attention. We use this nomenclature to differentiate it from feature-based attention, in which a relevant feature is used to select what object or location to attend to (e.g., attend to the red object). In feature-based attention, attention is directed toward objects and/or locations matching a cued value (e.g., red), while objects of a dif-

ferent color are ignored. In feature-selective attention, attention is instead directed toward a particular stimulus dimension (e.g., color), in preference to other dimensions (e.g., shape), to make a judgment about the relevant feature of a stimulus (Chen et al., 2012).

The adaptive coding hypothesis (Duncan, 2001) offers a possible neural mechanism for feature-selective attention. It holds that, within higher cortical regions, the response properties of single neurons are highly adaptable such that, in any particular task context, many cells become tuned to code information that is currently relevant. Evidence of such “adaptive coding” comes primarily from single-unit work with non-human primates in which neurons in higher cortical regions have been shown to alter coding as needed for behavior (Stokes et al., 2013; Cromer, Roy, & Miller, 2010; Roy, Riesenhuber, Poggio, & Miller, 2010; Freedman & Assad, 2006; Freedman, 2001; Sakagami & Niki, 1994). For example, in a go/no-go discrimination task where the relevant feature of a cue changed between three task contexts (Sakagami & Niki, 1994), 72% of PFC neurons showed different responses during the cue period for each task condition. In another example, Roy et al. (2010) demonstrated that 24% of PFC neurons had a distinct firing rate in response to one category of visual stimuli over another. These neurons responded to the relevant

Macquarie University, Sydney, Australia

Figure 1. The stimulus set consisted of 16 spiky objects with eight objects on either side of two orthogonal category boundaries. Category boundaries were defined based on the length (horizontal axis) or orientation (vertical axis) of the third spike from the bottom on the left side of the object. Spike length and orientation were titrated on an individual-participant basis to equate the difficulty of categorization across the two dimensions.



Stimuli

Stimuli were abstract novel “spiky” objects created using custom MATLAB scripts (Op de Beeck, Baker, DiCarlo, & Kanwisher, 2006). The stimulus set consisted of 16 objects (Figure 1) in which one spike varied along two dimensions (its length and orientation). Participants learnt to discriminate between the 16 objects across two orthogonal decision boundaries (task contexts) based on the length and orientation dimensions. The relevant visual feature of the stimuli therefore varied depending on the current decision boundary. The stimuli were aligned so that the main stem of the objects appeared at an angle of $+37^\circ$ from vertical. During both the training and scanning sessions, the visual angle (VA) of the spiky object’s length along its main axis was 8.07° . Stimulus presentation was controlled by a PC running the Psychophysics Toolbox 3 package (Brainard, 1997) in MATLAB (The MathWorks, Inc, Natick, MA). Stimuli were presented at central fixation on a screen and viewed through a mirror mounted on the head coil in the scanner.

Titration Task Difficulty

Less than 1 week (1–7 days) before scanning, participants completed a behavioral testing session in which we titrated the discriminability of the stimuli to ensure that the length and orientation tasks were of comparable difficulty on an individual participant level. We started with a difference of 1.26° VA between the shortest and longest lengths of the spike and a maximum difference of 27.02° in the angle of orientation. After 192 trials, the range of

lengths or orientations in the stimulus set was adjusted if there was a significant difference in the participant’s RTs between the two tasks ($p < .05$). For this, we increased the difficulty of the task that had the lower average RT. This procedure was repeated until there was no difference in RT between the two task contexts, as assessed with Bayes factor (BF) analysis (Love et al., 2015) in each participant separately (BF < 1 taken as evidence for no difference between conditions; Dienes 2011). The difficulty of the orientation context was increased for 11 participants (the maximum angle decreased to 21.92° for six participants and 13.86° for five participants), and the difficulty of the length context was increased for five participants (the maximum difference in VA was decreased to 1.06° for two participants and 0.95° for three participants).

Procedure

Before titrating the stimuli, participants completed six blocks of practice trials to learn the task. Stimuli were initially presented for 400 msec until participants achieved $>80\%$ correct, after which objects were presented for 216 msec. Feedback (correct/incorrect) was presented after each response until participants achieved $>80\%$ performance, after which feedback (percent correct) was only given at the end of each block. Once participants reached a high performance level ($>80\%$ correct) in both task contexts, we then titrated the stimuli to ensure equal performance in RTs (as described above). During titration, participants only received feedback at the end of each block. Immediately before entering the scanner, participants

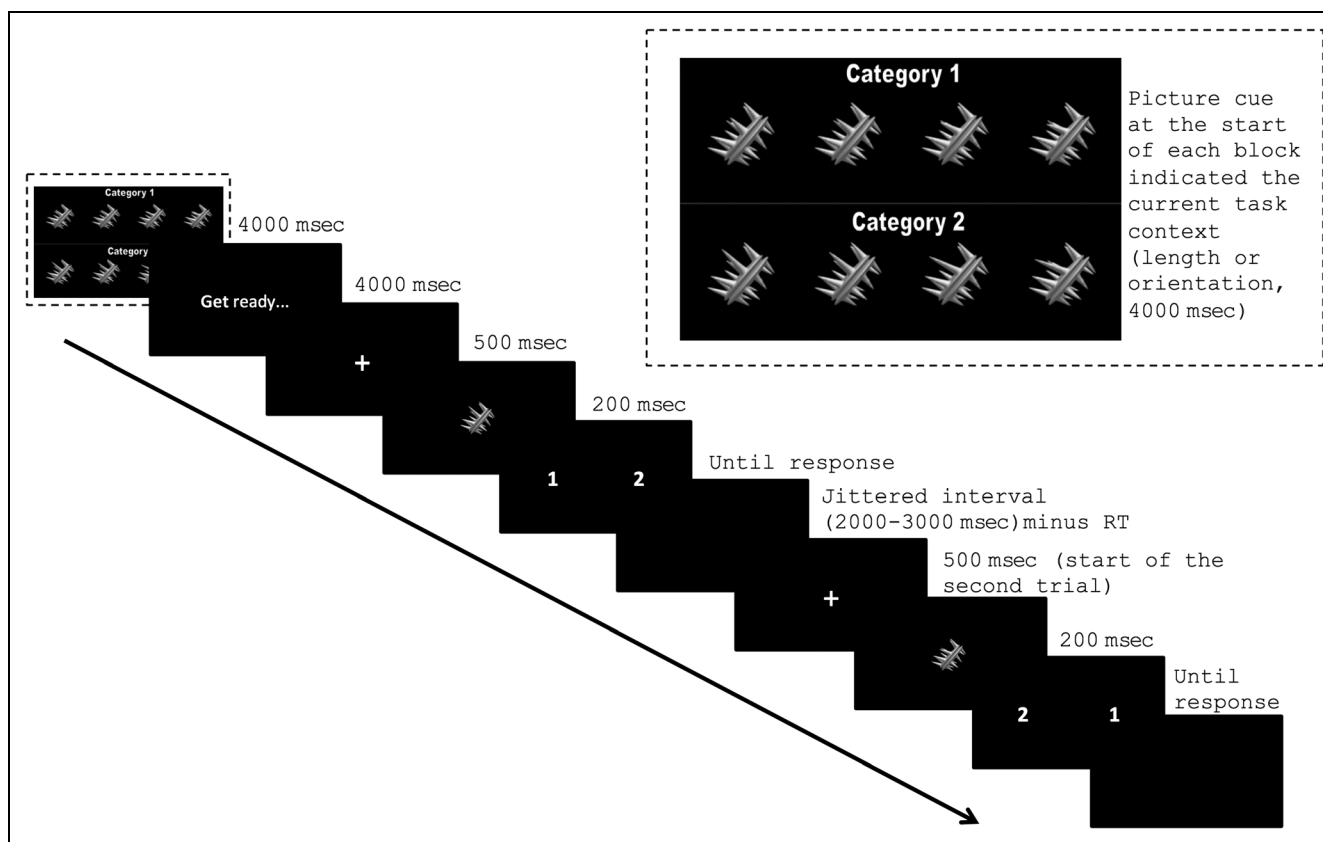


Figure 2. Stimulus categorization task: A picture cue at the start of each block indicated the current task context for categorization (orientation or length; inset shows cue display for the length task). On each trial, a fixation cross was presented for 500 msec followed by a spiky object for 200 msec. Finally, a response mapping screen appeared, which indicated the appropriate response button. In the example shown, the current context is length. For the first trial, the stimulus is Category 1 on the length dimension, and, therefore, the correct response was the left button.

completed a further two practice blocks of each task context to remind them of the task and to avoid initial practice effects in the scanner. These two practice blocks also introduced a response mapping screen to be used in the scanning task, which randomly assigned the button to be pressed for each category (short or long spikes in the length task and clockwise or anticlockwise spikes in the orientation task) on a trial-by-trial basis (Figure 2). This allowed separate estimation of the BOLD response associated with perceptual information about each category from that associated with each button press. Participants also performed an additional two practice blocks in the scanner during the structural scan, before commencing the main experiment, to familiarize them with the button-response box in the scanner.

Participants were scanned while performing the categorization task shown in Figure 2. Each participant completed four acquisition runs (8.09 min each) consisting of four blocks (32 trials/block), totaling 128 trials per acquisition run (2.02 min/block). At the start of each block, a picture cue (4000 msec) indicated the current task (length or orientation) and which attribute was Category 1 and 2 (e.g., whether short spikes/long spikes were Category 1 or 2; counterbalanced across participants). The order of

task contexts was counterbalanced across participants as well as within participants across runs. The picture cue depicted spiky objects from the extremes of the currently relevant dimension (see Figure 2, inset). The stimulus set was identical across the two contexts, but the relevant feature was either the length of the same spike relative to the category boundary or the orientation of a particular spike relative to the category boundary (rotated clockwise vs. anticlockwise from the boundary) in the different contexts. Thus, participants were attending to the same part of the object, but different features of that object part, in the two conditions. On each trial, participants saw a white central fixation cross (500 msec), after which the spiky object was presented at fixation for 216 msec. Finally, participants saw a response mapping screen, which indicated the category-to-button response mapping on this trial, and responded regarding the category membership of the stimulus. The response mapping screen randomly assigned Category 1 and 2 decisions to either the left or right response button, operated by the index or middle finger of the participant's right hand. The response mapping screen was visible until a button press was made or until the jittered time interval timed out (2000–3000 msec). If a response was made before the end of the intertrial

interval, a blank black screen was shown for the remainder of the trial time. Feedback (accuracy score) was presented at the end of each block for 6000 msec, after which there was a delay of 4000 msec before the start of the next block. At the end of each run, a blank black screen was shown for 4000 msec.

After completion of the main task during the scanning session, we ran a localizer task to functionally identify the LOC as an a priori ROI. Participants viewed central intact and scrambled versions of black and white common objects in 16.8-sec blocks of 16 trials (1100 msec/trial), while fixating on a central cross. Participants had to indicate via a button response when the fixation cross changed color to remind them to fixate centrally. There were 21 blocks consisting of alternating blocks of whole objects, scrambled objects, and rest blocks (counterbalanced across participants). The EPI (acquisition time) for the localizer task was 6.25 min.

Data Acquisition

The data were collected using a 3-T Verio Siemens (Erlangen, Germany) MRI scanner at Macquarie Medical Imaging, Macquarie University Hospital, Sydney, Australia. We used a sequential descending T2*-weighted EPI acquisition sequence with the following parameters: acquisition time = 2000 msec, echo time = 30 msec, 34 oblique axial slices with a slice thickness of 3.0 mm and a 0.70-mm interslice gap, in-plane resolution = 3.0×3.0 mm, matrix = 64×64 , field of view = 210 mm, and flip angle = 78° . T1-weighted magnetization prepared rapid gradient echo structural images were also acquired for all participants (slice thickness = 1.0 mm, resolution = 1.0×1.0 mm).

Preprocessing

MRI data were preprocessed using SPM 5 (Wellcome Department of Imaging Neuroscience, London, UK; www.fil.ion.ucl.ac.uk/spm) in MATLAB 2011b. Functional MRI data were converted from DICOM to NIFTII format, spatially realigned to the first functional scan and slice timing corrected, and structural images were co-registered to the mean EPI. EPIs from the main experiment were smoothed slightly (4-mm FWHM Gaussian kernel) to improve signal-to-noise ratio. LOC localizer EPIs were also smoothed (8-mm FWHM Gaussian kernel), and, in all cases, the data were high-pass filtered (128 sec). Structural scans were additionally normalized, using the segment and normalize routine of SPM5, to derive the individual participant normalization parameters needed for ROI definition (below).

ROIs

MD ROIs were defined using coordinates from a previous review of activity associated with a diverse set of cognitive demands (Duncan & Owen, 2000) using the kernel

method described in Cusack, Mitchell, and Duncan (2010), as in our previous work (Woolgar, Williams, et al., 2015; Woolgar, Hampshire, et al., 2011; Woolgar, Thompson, et al., 2011). The procedure yielded seven ROIs: left and right IFS (center of mass = $\pm 38, 26, 24$; volume = 17 cm^3), left and right AI/FO ($\pm 35, 19, 3$; 3 cm^3), left and right IPS ($\pm 35, -58, 41$; 7 cm^3), and ACC/pre-SMA ($0, 23, 39$; 21 cm^3).

Left and right visual cortex ROIs were derived from the Brodmann's template provided with MRICro (Rorden & Brett, 2000; Brodmann's area [BA] 17; center of mass = $-13, -81, 3/16, -79, 3$; volume = 54 cm^3). All coordinates are given in MNI152 space (McConnell Brain Imaging Centre, Montreal Neurological Institute). MD and BA 17 ROIs were deformed for each participant by applying the inverse of the participant's normalization parameters. This allowed analyses to be carried out using native space (i.e., nonnormalized) EPI data.

Using the functional localizer scan data, we defined LOC for each participant as the brain area that responded more strongly to whole objects than to scrambled versions of the same objects. We used the standard multiple regression approach of SPM5 (Wellcome Department of Imaging Neuroscience, London, UK; www.fil.ion.ucl.ac.uk) to estimate values pertaining to the whole and scrambled object conditions (block design). Blocks were modeled using a box car function lasting 16 sec convolved with the hemodynamic response of SPM5. The run mean was included in the model as a covariate of no interest. Whole-brain analyses (paired *t* tests) compared voxelwise BOLD response in the two conditions (whole objects minus scrambled objects). The resulting map was thresholded such that there was at least one cluster with a minimum size of 20 voxels. These clusters were then imported into MarsBaR (Brett, Anton, Valabregue, & Poline, 2002), and those active voxel clusters close to anatomical LOC coordinates from previous studies (Grill-Spector, Kushnir, Hendler, & Malach, 2000; Grill-Spector et al., 1999) were selected to form the ROI.

First-level Model

To obtain estimated activation patterns for multivariate analysis, a general linear model was estimated for each participant using the realigned, slice-time-corrected, and smoothed native space EPIs using SPM5 (Wellcome Department of Imaging Neuroscience, London, UK; www.fil.ion.ucl.ac.uk). We classified each stimulus as either "short" or "long" on the length dimension and "rotated clockwise" or "rotated anticlockwise" relative to the category boundary on the orientation dimension. Trials were modeled as events of zero duration convolved with the hemodynamic response of SPM5. Each trial contributed to the estimation of two beta values, the relevant feature (short or long for length context blocks and clockwise or anticlockwise for orientation context blocks) and the irrelevant feature (short or long for orientation context blocks and clockwise

or anticlockwise for length context blocks). We derived the estimates for each feature in each block separately. The two run means were included in the model as covariates of no interest. Error trials were excluded from the analysis.

MVPA

We used MVPA to examine the representation of relevant and irrelevant stimulus features. Of central interest was whether the MD regions adapted to code length and orientation information more strongly when it was relevant for the task than when it was task irrelevant. We also examined the same stimulus feature distinctions in the LOC and early visual cortex (BA 17).

We implemented MVPA using the Decoding Toolbox (Hebart, Görger, & Haynes, 2015), which wraps the LIBSVM library (Chang & Lin, 2011). We examined coding of orientation when orientation was relevant, orientation when orientation was irrelevant, length when length was relevant, and length when length was irrelevant. For each participant and ROI, a linear support vector machine was trained to decode the relevant (clockwise/anticlockwise in orientation blocks and short/long in length blocks) and irrelevant (clockwise/anticlockwise in length blocks and short/long in orientation blocks) stimulus features for each task context separately. In total, there were 16 blocks for each participant: eight with relevant length and eight with relevant orientation. For each classification, we used a leave-one-out eight-fold splitter whereby the classifier was trained using the data from seven of the eight blocks and subsequently tested on its accuracy at classifying the unseen data from the remaining block, iterating over all possible combinations of training and testing blocks. For example, to yield a classification accuracy score for the task-relevant length distinctions, we took the eight blocks in which participants performed the length task and trained the classifier to distinguish between patterns of activation representing short and long spikes in seven of these eight blocks and then tested generalization to the remaining unseen block. The accuracies were then averaged to give a mean accuracy score for task-relevant length coding. This was repeated for each condition, participant, and ROI separately.

The mean classification accuracy for each participant in each ROI and in each condition was then entered into a second level analysis. Of central interest was whether the MD network would code task-relevant stimulus features more strongly than task-irrelevant ones. To address this, we conducted a three-factor ANOVA on classifier accuracy with the factors Relevancy, Feature, and MD region. To explore any hemispheric effects, we ran an additional ANOVA with factors Relevancy, Feature, MD region, and Hemisphere.

Because a difference in coding between relevant and irrelevant conditions is only interpretable if coding in at least one condition is also significantly above chance, we also conducted one-sample *t* tests against the classifica-

tion accuracy expected by chance (50%) in each condition (relevant and irrelevant) separately. One-tailed significance tests were used where appropriate for inference: Tests comparing classification of relevant with irrelevant feature distinctions in the MD regions are one tailed because the direction of the effect is prespecified, and tests comparing classification accuracy with chance are one tailed as below-chance classifications are not interpretable. All other tests are two tailed. Alpha was adjusted for four comparisons using Bonferroni correction (.05 divided by 4).

We also examined whether coding in the visual cortices was stronger for task-relevant than task-irrelevant stimulus features. For this, we used a two-factor ANOVA on classifier accuracy with factors Relevancy (task relevant, task irrelevant) and Feature (orientation, length) for each of the visual cortex ROIs (LOC, early visual cortex) collapsed across hemispheres. Again, we also tested whether coding in the visual cortices was above chance in each condition separately (one-sample *t* test against the classification accuracy expected by chance, 50%).

We conducted an additional analysis in which the classifier was trained on data representing the category number decisions in one task context (Category 1 or 2) and tested on the category number decisions participants made in the other task context (Category 1 or 2). We included this analysis to explore whether the categorization decision was represented at the level of the stimulus (i.e., short/long) or at the level of the category number (Category 1 or 2).

Finally, in addition to the standard parametric statistics outlined above, we conducted a two-step permutation test (Stelzer, Chen, & Turner, 2013) to compare coding of relevant and irrelevant information to chance and coding of relevant and irrelevant information to each other, in a nonparametric framework. For each decoding analysis (e.g., short/long in length blocks), each ROI, and each person, we exhaustively permuted the class labels within each block (128 combinations) and trained and tested the classifier on each permutation. Next, we built three group-level null distributions, one for relevant information (short/long in length blocks and clockwise/anticlockwise in orientation blocks), one for irrelevant information (short/long in orientation blocks and clockwise/anticlockwise in length blocks), and one for the difference between relevant and irrelevant information (relevant minus irrelevant). Each null distribution was created by sampling (with replacement) 10,000 times from the set of participants \times 128 relevant permutation classification results (one sample per participant per iteration, single-participant data collapsed permutation-wise over length and orientation). Finally, we calculated the probability *p* of observing each decoding accuracy (from the correctly labeled data) given the relevant group null distribution, using the Monte-Carlo approach (Hammersley, 2013), in which $p = (k + 1) / (n + 1)$ where *k* is the number of permutations in the group null with equal or higher accuracy to the actual value and *n* is the number

region. Furthermore, BA 17 did not show categorical discrimination of these visually similar objects according to either the task-relevant (relative to chance; mean classification accuracy = 52.91%, $t(25) = 1.62$, $p = .14$) or task-irrelevant (relative to chance; mean classification accuracy = 52.31%, $t(25) = 1.17$, $p = .25$) stimulus features. The two-step permutation tests similarly showed no evidence that BA 17 coded the task-relevant over the task-irrelevant features ($p = .41$). In addition, coding of relevant ($p = .08$) and irrelevant ($p = .12$) features did not reach significance. As the stimuli were identical in the different task contexts, it is not at all surprising to find that the early visual cortex information does not distinguish between these stimuli, although, as with all null effects, we must be cautious about interpretation.

Coding of Category Placement

On each trial, participants had to categorize the object according to the relevant feature dimension (e.g., short/long on length blocks), associate that decision with the number representing the chosen category (1 or 2, e.g., short = 1 in half of the participants), and then use the response mapping screen to transform their choice into the appropriate button press response (left or right, 1 = left in half of the trials). Therefore, it is possible that, as well as the categorization decision at the level of the stimulus, participants also held a category number in mind on each trial. To test for representation at this higher level of abstraction, we ran an additional analysis where we trained the classifier on the data representing the category number decisions in one task context and tested this on the category number decisions participants made in the other task context. We were not able to decode the category number placement of the objects in the MD system (mean classification accuracy = 50.54%, $t(25) = 1.31$, $p = .21$). To interpret this null effect, we calculated the BF. Coding of category number placement revealed a BF_{10} of 0.44. As this is less than 1 (Dienes, 2011) and approaches the level of 0.33 suggested by Jeffreys (1998) to represent significant evidence for the null hypothesis, we interpret this as evidence that, although the MD regions encode task-relevant stimulus distinctions, the representation is not abstracted to the level of categorical number placement.

DISCUSSION

The adaptive coding hypothesis (Duncan, 2001) proposes that neural populations dynamically adjust their responses to selectively code information that is currently relevant for our behavior. This provides a possible mechanism for feature-selective attention, which allows information about task-relevant stimulus features to be processed in preference to irrelevant attributes. We examined the responses of the MD regions in a difficult visual object

categorization task in which the relevant stimulus dimension varied on physically identical stimuli. The MD system adjusted its representation of these novel objects to preferentially encode feature distinctions that were relevant for the task. When the task required participants to categorize the objects based on length, the MD regions coded length information more strongly than orientation information, but when the task was to categorize based on orientation, orientation was encoded in preference to length. Thus, the MD system adjusted its representation of the features of an object to encode the discrimination necessary for the current task. Consistent with the proposal that the cognitive flexibility of these regions underlies their involvement in a wide range of tasks (e.g., Duncan, 2010; Cole & Schneider, 2007; Duncan & Owen, 2000), our data suggest that the coding of this adaptive system adjusts to hold the currently relevant features of a stimulus as needed for behavior.

Electrophysiology studies in nonhuman primates have previously shown that neurons in higher cortical regions adapt their tuning profiles to respond most strongly to the information that is currently relevant (Stokes et al., 2013; Cromer et al., 2010; Roy et al., 2010; Freedman & Assad, 2006; Freedman, 2001; Sakagami & Niki, 1994). The implementation of MVPA for fMRI has shown similar results in humans: Patterns of activation in the MD regions code a range of different types of task-related information (e.g., Woolgar, Williams, et al., 2015; Nee & Brown, 2012; Reverberi et al., 2011; Woolgar, Hampshire, et al., 2011; Woolgar, Thompson, et al., 2011; Bode & Haynes, 2009; Haynes et al., 2007; Li et al., 2007) and adjust their responses when task demands vary (Woolgar, Afshar, et al., 2015; Woolgar, Williams, et al., 2015; Woolgar, Hampshire, et al., 2011; Li et al., 2007). The MD regions also encode attended objects in preference to unattended objects (Woolgar, Williams, et al., 2015), and a previous adaptation study demonstrated that these regions show greater responses to changes in attended stimulus features (color/shape) than to changes in unattended stimulus features (Thompson & Duncan, 2009). Here, we find that these regions can also flexibly adapt their representations of single objects to emphasize task-relevant stimulus distinctions, resulting in preferential coding of attended stimulus features.

Our data align with a recent study in which objects were strongly represented in LPFC in individual task contexts, but the representation did not generalize between task contexts (Harel et al., 2014). Those data suggested that the same set of objects may be represented differently as task contexts change. Here, we tested this possibility directly by specifying the specific stimulus distinctions that an adaptive system should make in each task context. We found that the MD system adjusted its representation of the set of novel objects to make the specific distinctions needed for the task. In a related study (Peelen & Caramazza, 2012), participants responded to one of two semantic dimensions of an object (how the object is used or where the object is found) in a 1-back task. Results from a

- Brett, M., Anton, J., Valabregue, R., & Poline, J. (2002). Region of interest analysis using an SPM toolbox. *Neuroimage*, *16*, S497.
- Chang, C. C., & Lin, C. J. (2011). LIBSVM: A library for support vector machines. *ACM Transactions on Intelligent Systems and Technology*, *2*, 27.
- Chen, X., Hoffmann, K. P., Albright, T. D., & Thiele, A. (2012). Effect of feature-selective attention on neuronal responses in macaque area MT. *Journal of Neurophysiology*, *107*, 1530–1543.
- Cole, M. W., Reynolds, J. R., Power, J. D., Repovs, G., Anticevic, A., & Braver, T. S. (2013). Multi-task connectivity reveals flexible hubs for adaptive task control. *Nature Neuroscience*, *16*, 1348–1355.
- Cole, M. W., & Schneider, W. (2007). The cognitive control network: Integrated cortical regions with dissociable functions. *Neuroimage*, *37*, 343–360.
- Corbetta, M., Akbudak, E., Conturo, T. E., Snyder, A. Z., Ollinger, J. M., Drury, H. A., et al. (1998). A common network of functional areas for attention and eye movements. *Neuron*, *21*, 761–773.
- Cromer, J. A., Roy, J. E., & Miller, E. K. (2010). Representation of multiple, independent categories in the primate prefrontal cortex. *Neuron*, *66*, 796–807.
- Culham, J. C., Cavanagh, P., & Kanwisher, N. G. (2001). Attention response functions: Characterizing brain areas using fMRI activation during parametric variations of attentional load. *Neuron*, *32*, 737–745.
- Cusack, R., Mitchell, D. J., & Duncan, J. (2010). Discrete object representation, attention switching, and task difficulty in the parietal lobe. *Journal of Cognitive Neuroscience*, *22*, 32–47.
- Dienes, Z. (2011). Bayesian versus orthodox statistics: Which side are you on? *Perspectives on Psychological Science*, *6*, 274–290.
- Dosenbach, N. U. F., Visscher, K. M., Palmer, E. D., Miezin, F. M., Wenger, K. K., Kang, H. C., et al. (2006). A core system for the implementation of task sets. *Neuron*, *50*, 799–812.
- Duncan, J. (2001). An adaptive coding model of neural function in prefrontal cortex. *Nature Reviews Neuroscience*, *2*, 820–829.
- Duncan, J. (2010). The multiple-demand (MD) system of the primate brain: Mental programs for intelligent behaviour. *Trends in Cognitive Sciences*, *14*, 172–179.
- Duncan, J., & Owen, A. M. (2000). Common regions of the human frontal lobes recruited by diverse cognitive demands. *Trends in Cognitive Sciences*, *23*, 475–483.
- Ester, E. F., Sprague, T. C., & Serences, J. T. (2015). Parietal and frontal cortex encode stimulus-specific mnemonic representations during visual working memory. *Neuron*, *87*, 893–905.
- Fedorenko, E., Duncan, J., & Kanwisher, N. G. (2013). Broad domain-generalty in focal regions of frontal and parietal cortex. *Proceedings of the National Academy of Sciences, U.S.A.*, *110*, 16616–16621.
- Fox, M. D., Snyder, A. Z., Vincent, J. L., Corbetta, M., Van Essen, D. C., & Raichle, M. E. (2005). From the cover: The human brain is intrinsically organized into dynamic, anticorrelated functional networks. *Proceedings of the National Academy of Sciences, U.S.A.*, *102*, 9673–9678.
- Freedman, D. J. (2001). Categorical representation of visual stimuli in the primate prefrontal cortex. *Science*, *291*, 312–316.
- Freedman, D. J., & Assad, J. A. (2006). Experience-dependent representation of visual categories in parietal cortex. *Nature*, *443*, 85–88.
- Grill-Spector, K., Kourtzi, Z., & Kanwisher, N. G. (2001). The lateral occipital complex and its role in object recognition. *Vision Research*, *21*, 1409–1422.
- Grill-Spector, K., Kushner, T., Edelman, S., Avidan, G., Itzhak, Y., & Malach, R. (1999). Differential processing of objects under various viewing conditions in the human lateral occipital complex. *Neuron*, *24*, 187–203.
- Grill-Spector, K., Kushnir, T., Hendler, T., & Malach, R. (2000). The dynamics of object-selective activation correlate with recognition performance in humans. *Nature Neuroscience*, *3*, 837–843.
- Hammersley, J. (2013). *Monte Carlo methods*. Berlin, Germany: Springer Science & Business Media.
- Harel, A., Kravitz, D., & Baker, C. I. (2014). Task context impacts visual object processing differentially across the cortex. *Proceedings of the National Academy of Sciences, U.S.A.*, *111*, E962–E971.
- Haxby, J. V., Gobbini, M. I., Furey, M. L., Ishai, A., Schouten, J. L., & Pietrini, P. (2001). Distributed and overlapping representations of faces and objects in ventral temporal cortex. *Science*, *293*, 2425–2429.
- Haynes, J. D., & Rees, G. (2005). Predicting the orientation of invisible stimuli from activity in human primary visual cortex. *Nature Neuroscience*, *8*, 686–691.
- Haynes, J.-D., Sakai, K., Rees, G., Gilbert, S., Frith, C., & Passingham, R. E. (2007). Reading hidden intentions in the human brain. *Current Biology*, *17*, 323–328.
- Hebart, M. N., Gorgen, K., & Haynes, J.-D. (2015). The Decoding Toolbox (TDT): A versatile software package for multivariate analyses of functional imaging data. *Frontiers in Neuroinformatics*, *8*, 88. doi:10.3389/fninf.2014.00088
- Jeffreys, H. (1998). *The theory of probability*. Oxford, UK: OUP Oxford.
- Jehee, J. F. M., Brady, D. K., & Tong, F. (2011). Attention improves encoding of task-relevant features in the human visual cortex. *Journal of Neuroscience*, *31*, 8210–8219.
- Jerde, T. A., Merriam, E. P., Riggall, A. C., Hedges, J. H., & Curtis, C. E. (2012). Prioritized maps of space in human frontoparietal cortex. *Journal of Neuroscience*, *32*, 17382–17390.
- Kadohisa, M., Petrov, P., Stokes, M., Sigala, N., Buckley, M., Gaffan, D., et al. (2013). Dynamic construction of a coherent attentional state in a prefrontal cell population. *Neuron*, *80*, 235–246.
- Kamitani, Y., & Tong, F. (2005). Decoding the visual and subjective contents of the human brain. *Nature Neuroscience*, *8*, 679–685.
- Kok, P., Jehee, J. F. M., & de Lange, F. P. (2012). Less is more: Expectation sharpens representations in the primary visual cortex. *Neuron*, *75*, 265–270.
- Konen, C. S., & Kastner, S. (2008). Two hierarchically organized neural systems for object information in human visual cortex. *Nature Neuroscience*, *11*, 224–231.
- Li, S., Ostwald, D., Giese, M., & Kourtzi, Z. (2007). Flexible coding for categorical decisions in the human brain. *Journal of Neuroscience*, *27*, 12321–12330.
- Love, J., Selker, R., Marsman, M., Jamil, T., Dropmann, D., Verhagen, A. J., et al. (2015). *JASP (Version 0.7) [computer software]*. Amsterdam, The Netherlands: JASP Project.
- Mante, V., Sussillo, D., Shenoy, K. V., & Newsome, W. T. (2013). Context-dependent computation by recurrent dynamics in prefrontal cortex. *Nature*, *503*, 78–84.
- Murray, S. O., & He, S. (2006). Contrast invariance in the human lateral occipital complex depends on attention. *Current Biology*, *16*, 606–611.
- Murray, S. O., & Wojciulik, E. (2003). Attention increases neural selectivity in the human lateral occipital complex. *Nature Neuroscience*, *7*, 70–74.
- Nee, D. E., & Brown, J. W. (2012). Rostral-caudal gradients of abstraction revealed by multi-variate pattern analysis of working memory. *Neuroimage*, *63*, 1285–1294.

- Nyberg, L., Marklund, P., Persson, J., Cabeza, R., Forkstam, C., Pettersson, K. M., et al. (2003). Common prefrontal activations during working memory, episodic memory, and semantic memory. *Neuropsychologia*, *41*, 371–377.
- Op de Beeck, H. P., Baker, C. I., DiCarlo, J. J., & Kanwisher, N. G. (2006). Discrimination training alters object representations in human extrastriate cortex. *Journal of Neuroscience*, *26*, 13025–13036.
- Peelen, M. V., & Caramazza, A. (2012). Conceptual object representations in human anterior temporal cortex. *Journal of Neuroscience*, *32*, 15728–15736.
- Reverberi, C., Gorgen, K., & Haynes, J. D. (2011). Compositionality of rule representations in human prefrontal cortex. *Cerebral Cortex*, *22*, 1237–1246.
- Rorden, C., & Brett, M. (2000). Stereotaxic display of brain lesions. *Behavioural Neurology*, *12*, 191–200.
- Roy, J. E., Riesenhuber, M., Poggio, T., & Miller, E. K. (2010). Prefrontal cortex activity during flexible categorization. *Journal of Neuroscience*, *30*, 8519–8528.
- Sakagami, M., & Niki, H. (1994). Encoding of behavioral significance of visual stimuli by primate prefrontal neurons: Relation to relevant task conditions. *Experimental Brain Research*, *97*, 423–436.
- Stelzer, J., Chen, Y., & Turner, R. (2013). Statistical inference and multiple testing correction in classification-based multi-voxel pattern analysis (MVPA): Random permutations and cluster size control. *Neuroimage*, *65*, 69–82.
- Stokes, M. G., Kusunoki, M., Sigala, N., Nili, H., Gaffan, D., & Duncan, J. (2013). Dynamic coding for cognitive control in prefrontal cortex. *Neuron*, *78*, 364–375.
- Thompson, R., & Duncan, J. (2009). Attentional modulation of stimulus representation in human frontoparietal cortex. *Neuroimage*, *48*, 436–448.
- Vincent, J. L., Kahn, I., Snyder, A. Z., Raichle, M. E., & Buckner, R. L. (2008). Evidence for a frontoparietal control system revealed by intrinsic functional connectivity. *Journal of Neurophysiology*, *100*, 3328–3342.
- Woolgar, A., Afshar, S., Williams, M. A., & Rich, A. N. (2015). Flexible coding of task rules in frontoparietal cortex: An adaptive system for flexible cognitive control. *Journal of Cognitive Neuroscience*, *27*, 1895–1911.
- Woolgar, A., Hampshire, A., Thompson, R., & Duncan, J. (2011). Adaptive coding of task-relevant information in human frontoparietal cortex. *Journal of Neuroscience*, *31*, 14592–14599.
- Woolgar, A., Thompson, R., Bor, D., & Duncan, J. (2011). Multi-voxel coding of stimuli, rules, and responses in human frontoparietal cortex. *Neuroimage*, *56*, 744–752.
- Woolgar, A., Williams, M. A., & Rich, A. N. (2015). Attention enhances multi-voxel representation of novel objects in frontal, parietal and visual cortices. *Neuroimage*, *109*, 429–437.
- Xu, Y., & Chun, M. M. (2005). Dissociable neural mechanisms supporting visual short-term memory for objects. *Nature*, *440*, 91–95.